



Discovery of selective and orally available spiro-3-piperidyl ATP-competitive MK2 inhibitors

Allard Kaptein, Arthur Oubrie, Edwin de Zwart, Niels Hoogenboom, Joeri de Wit, Bas van de Kar, Maaike van Hoek, Gerard Vogel, Vera de Kimpe, Carsten Schultz-Fademrecht, Judith Borsboom, Mario van Zeeland, Judith Versteegh, Bert Kazemier, Jeroen de Roos, Frank Wijnands, John Dulos, Martin Jaeger, Paula Leandro-Garcia, Tjeerd Barf*

Merck Research Laboratories, MSD, PO Box 20, 5340 BH Oss, The Netherlands

ARTICLE INFO

Article history:

Received 11 February 2011

Revised 29 March 2011

Accepted 3 April 2011

Available online 16 April 2011

Keywords:

MAPKAPK2

MK2

Anti-TNF α

Oral bioavailability

Rheumatoid arthritis

ABSTRACT

The identification of a potent, selective, and orally available MK2 inhibitor series is described. The initial absence of oral bioavailability was successfully tackled by moving the basic nitrogen of the spiro-4-piperidyl moiety towards the electron-deficient pyrrolopyridinedione core, thereby reducing the pK_a and improving Caco-2 permeability. The resulting racemic spiro-3-piperidyl analogues were separated by chiral preparative HPLC, and the activity towards MK2 inhibition was shown to reside mostly in the first eluting stereoisomer. This led to the identification of new MK2 inhibitors, such as (*S*)-**23**, with low nanomolar biochemical inhibition (EC_{50} 7.4 nM) and submicromolar cellular target engagement activity (EC_{50} 0.5 μ M).

© 2011 Elsevier Ltd. All rights reserved.

The p38-MK2 signaling pathway is crucial for activation of pro-inflammatory cytokines in response to stress signals including pro-inflammatory cytokines, bacterial lipopolysaccharide (LPS) and hypoxia.¹ The pathway plays a central role in pathogenic cellular mechanisms of rheumatoid arthritis (RA) and other related autoimmune diseases. Drug discovery on p38 has resulted in several inhibitors that have progressed to phase 2 in the clinic. Drug toxicity, lack of efficacy and activation of other inflammatory signaling pathways following p38 inhibition, have hampered progression to phase 3 clinical trials.² MK2 is downstream of p38 and an attractive alternative drug discovery target for the p38-MK2 signaling pathway, also given the anti-TNF α phenotype of MK2 deficient mice.³

Profiles of several ATP-competitive chemotypes have been published, and these have been reviewed recently.⁴ One of the reported scaffolds is the pyrrolopyridinone class of MK2 inhibitors as exemplified by PH-089 (Fig. 1).⁵ Proof of principle has been demonstrated with this orally available MK2 inhibitor, but the in vitro and in vivo activity is limited for this compound. As previously reported, introduction of a 4-piperidyl moiety on the pyrrolopyridinone scaffold gave a substantial improvement in biochemical and cellular activity as well as in solubility.⁶ However,

4-piperidyl-based MK2 inhibitors suffered from a lack of oral bioavailability ($F = 0.7\%$ (po) in mice). Following iv or sc administration, compound **1** showed significant inhibition of LPS-induced TNF α at 12.5 and 30 mg/kg in rats, respectively. Thus, exposure of **1** was sufficient to achieve in vivo efficacy with these administration routes.

With compound **1** as the early lead, we set out to identify analogues that combine MK2 inhibitory activity with favorable ADME parameters. The general preparation of the inhibitors is outlined in Scheme 1, and an optimized route as compared to that described in an earlier report.⁶ On the commercially Boc-protected piperidine **A**, a trimethoxybenzyl group (TMB) was introduced via a reductive amination. It was advantageous to protect the primary amine function with a TMB group, since this sterically demanding group facilitated the Dieckmann condensation step. It forces the attacking malonyl carbanion in close proximity to the reacting methyl ester

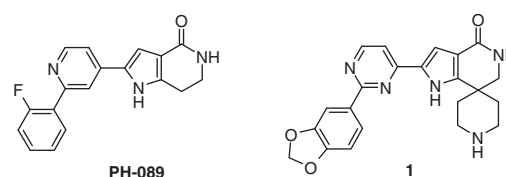
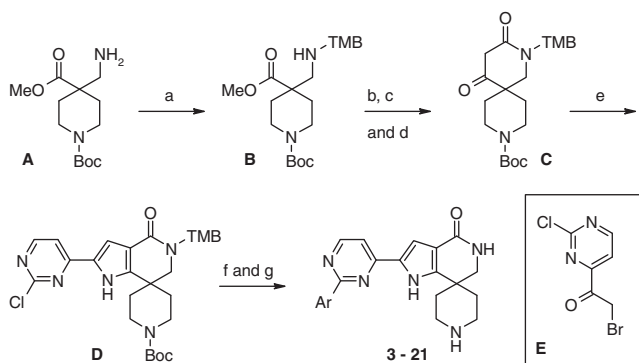


Figure 1. Pyrrolopyridinone PH-089 and compound **1**.

* Corresponding author. Tel.: +31 412 661768; fax: +31 412 662546.

E-mail address: tjeerd.barf@merck.com (T. Barf).



Scheme 1. Reagents and conditions: (a) 2,4,6-trimethoxybenzaldehyde, NaB-H(OAc)₃, EtOH, rt (100%); (b) ClCOCH₂COOEt, DMAP, pyridine, DCM, rt (100%); (c) NaOMe, MeOH, 60 °C (100%); (d) ACN/H₂O (1:1) 80 °C (98%); (e) Compd E, NH₄OAc, EtOH (35%); (f) arylboronic acid, PdCl₂ (dppf), K₃PO₄·7H₂O, dioxane, 140 °C, MW; (g) TFA, rt (4–48% in two steps).

group on the bridgehead resulting in drastically improved isolated yields. Also, it provided UV-positive intermediates that were easy to track during the workup and purification stages. Acylation with ethyl (chloroformyl)acetate, a Dieckmann condensation and decarboxylation subsequently rendered intermediate **C**. Paal–Knorr condensation was carried out with chloropyrimidine derivative **E** (see insert *Scheme 1*),⁶ followed by a Suzuki-coupling to introduce the various aryl moieties in the front pocket. Final compounds were generated by a one-step acidic removal of the Boc- and TMB-protective groups. The N-alkylated analogues **3b** and **3c** were synthesized via standard reductive amination procedures on the unsubstituted 4-piperidyl parent molecule **3a**.

The basic amine function seems to be a prerequisite for MK2 inhibitory activity, since the direct pyrane analogue **2** demonstrates a 180-fold drop in activity (*Table 1*).⁷ Benzofurane derivative **3a** was equipotent to the methylenedioxyphenyl substitution, but the higher cellular potency observed in the TNF α production in THP1 and PBMC cells could not be confirmed in the Hsp27 phosphorylation target engagement assay (pHsp27). N-Alkylation of the 4-piperidyl moiety with a methyl (**3b**) or ethyl (**3c**) in the benzofurane series resulted in a 2- and 10-fold loss in biochemical potency. As for **3a**, the cellular THP1 readouts did not correlate very well. Plotting the target engagement (pHsp27) and cytokine production (TNF α) EC₅₀ values in THP1 cells, the high overall correlation of these two parameters becomes evident (*Fig. 2*). This graph also clearly shows that the benzofurane-derived MK2 inhibitors belong to the few outliers. There is a 4- to 10-fold difference in EC₅₀ values obtained in the pHsp27 and TNF α assays, while all other compounds are within a 2-fold difference from equipotency on both parameters. This suggests that a promiscuous component aids to the inhibition of LPS-induced cytokine production in THP1 cells. Since the benzofuranyl series did not reveal any cytotoxicity in THP1 cells, as determined with Alamar Blue in concert with cytokine production (>10 μ M for **3a–3c**; data not shown), off-target contribution to the overall efficacy on LPS-induced TNF α production is anticipated for this particular subseries. The potential to inhibit p38 was routinely monitored for these analogues, and no substantial inhibition was observed (data not shown).

While screening for additional substituents on the (hetero)-aryl portion in the front pocket, it became evident that the nature of properties that are accepted in this region is very diverse (*Table 1*). Hydrogen bond accepting (**4**, **15–17**) as well as donating substituents (**18–21**) are allowed. Also, small lipophilic groups on the *meta* position, or bulkier aliphatic groups on the *para* position can be beneficial. In sharp contrast, ortho substitution is not allowed except for fluorine as in **8**, showing that co-planarity of

the (hetero)-aryl and the pyrimidyl is essential for proper binding to the hinge and front pocket regions. Despite the low nanomolar biochemical potency of many of these compounds, substantial cellular inhibition was only obtained if the lipophilicity was above a certain level ($c \log P > 1$). Examples **16–20** are probably not sufficiently lipophilic to produce a decent cellular effect. Introduction of aliphatic groups, such as a cyclopentyl in **21** (as compared to unsubstituted **20**), restored the cellular activity somewhat. Increased lipophilicity did not necessarily correlate with membrane permeability as determined in our PAMPA and Caco-2 assays, and permeability properties were disappointingly low for all 4-piperidyl analogues (*Table 2*).

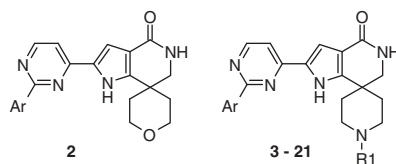
We reasoned that the lack of permeability could be the prime cause of both low cellular activity and absence of oral bioavailability in this series, as the microsomal and hepatocyte stabilities of our MK2 inhibitors were generally very good (*Table 2*). The basicity of the unsubstituted 4-piperidyl moiety was determined experimentally; the pK_a's of **1** and **3a** were 9.3 and 9.1, respectively (*Table 2*). We therefore sought to lower the basicity with the aim to improve the above mentioned parameters. In general, pK_a values can potentially be reduced via introduction of (electron-withdrawing) aliphatic substituents. Another, less conventional possibility, was to move the basic nitrogen closer to the electron-deficient pyrrole ring. By doing so, a net electron-withdrawing effect could lower the pK_a. Consistent with this hypothesis, the calculated log *P* values of 4- and 3-piperidyl analogues with identical molecular formulas differed on average by 0.3–0.4 log unit (compare e.g., **1** and **23**, and **3a** and **22** in *Table 3*).

Preparation of the 3-piperidyl analogues started with iodomethylation of commercially available **F** (*Scheme 2*). Subsequent nucleophilic substitution with sodium azide, and reduction to the primary amine gave intermediate **H**. Reductive N-alkylation with trimethoxybenzaldehyde, and construction of the oxolactam ring according to the methods described for the 4-piperidyl derivatives, furnished intermediate **K**. Final test compounds were again prepared in analogy of *Scheme 1*.

Compared to their basic amine containing equivalents, N-alkyl analogues **3b** (Me) and **3c** (Et) exhibited higher lipophilicity, lower pK_a values and improved Caco-2 permeability at the expense of biochemical activity (*Table 2*). This appeared to only marginally improve oral exposure in rats, at least within the benzofuranyl series, when comparing the 4-piperidyl NH (AUC <0.006 μ M h), N-Me (0.078 μ M h), N-Et (0.154 μ M h). A substantial improvement in oral exposure in this series was obtained through the 3-piperidyl (0.472 μ M h) analogue. This trend towards improved oral bioavailability was also observed in many other 3-piperidyl analogues, for example, **23** and **25**. For these compounds, Caco-2 permeabilities exceeded 20 nm/s, and the pK_a values ranged from 8.2 to 8.4. There is a fairly good correlation between lower pK_a values, increased permeability and improved oral exposure following rapid rat pharmacokinetic experiments. The biochemical EC₅₀ values of the 3-piperidyl analogues were somewhat compromised, but this is more than compensated for by this series' PK properties: The AUC in rats after oral administration of **23** was 3.2 μ M h along with acceptable half lives in human and rat liver microsomes. The oral bioavailability of **23** was confirmed in mice and with *F* = 48% (AUC = 3.5 μ M h) its oral exposure is superior to that of **1** (*F* = 0.7%). Also, the cellular activities as shown by both pHsp27 and TNF α inhibition EC₅₀ values are still in the low micromolar range (*Table 3*, compounds **23–26**) and comparable to 4-piperidyl analogue **1**.

The generation of 3-piperidyl analogues provided another interesting avenue, namely separating and testing of enantiomers. This often provides increased potency, and could generate additional proof as to whether MK2 inhibition is indeed correlated with cellular inhibition of pHsp27 and TNF α in THP1 cells. A couple of

Table 1
Inhibitory MK2 activity of compounds **1–21**



Compd	Ar	R1	MK2 IMAP EC ₅₀ ^a (nM)	TNF EC ₅₀ ^b (μM)	pHsp27 EC ₅₀ ^c (μM)
PH-089	—	—	372	9.1	2.7
1	3,4(-OCH ₂ O-)C ₆ H ₃	H	4.3	0.91	0.62
2	3,4(-OCH ₂ O-)C ₆ H ₃	—	724	>10	NT ^d
3a	Benzofuran-2-yl	H	5.9	0.28	1.2
3b	Benzofuran-2-yl	Me	13	0.47	1.6
3c	Benzofuran-2-yl	Et	59	1.6	>10
					<i>c</i> Log <i>P</i>
4	3-(COMe)C ₆ H ₄	H	11	6.2	1.1
5	4-(COMe)C ₆ H ₄	H	9.8	5.0	1.1
6	3,4(-O(CH ₂) ₃ O-)C ₆ H ₃	H	10	4.9	1.8
7	3-(<i>i</i> Pr)C ₆ H ₄	H	112	>10	3.1
8	2-FC ₆ H ₄	H	29	4.2	1.8
9	3-FC ₆ H ₄	H	8.3	1.4	1.8
10	3-(CF ₃)C ₆ H ₄	H	15	4.2	2.5
11	4-(CF ₃)C ₆ H ₄	H	6.9	6.3	2.5
12	4-(<i>t</i> Bu)C ₆ H ₄	H	6.2	5.9	3.5
13	Naphth-2-yl	H	5.1	3.6	2.8
14	3,5-Di-ClC ₆ H ₃	H	4.5	6.3	3.1
15	Quinolin-3-yl	H	6.3	4.8	1.6
16	Pyrid-3-yl	H	1.1	>10	0.2
17	5-MeO-pyrid-3-yl	H	6.9	>10	0.7
18	6-NH ₂ -pyrid-3-yl	H	15	>10	0
19	6-NHCOEt-pyrid-3-yl	H	3.6	>10	0.7
20	2-NH ₂ pyrimid-5-yl	H	2.1	>10	-0.7
21	2- <i>c</i> PentNHpyrimid-5-yl	H	1.7	2.6	1.6

^a Values are means of two independent experiments with duplicates for each dilution per experiment. For experimental details see Ref. 6.

^b THP1 cells are pre-incubated for 30 min with MK2 inhibitors (duplicates for each dilution) prior to stimulation with LPS. Four hours following LPS induction culture medium is withdrawn from the cells for TNFα measurements. For experimental details see Ref. 6.

^c THP1 cells are pre-incubated for 60 min with MK2 inhibitors (duplicates for each dilution) prior to stimulation with LPS. 10 min following LPS induction cells are lysed for measurement of Hsp27 and phospho-Hsp27.⁸

^d NT: not tested.

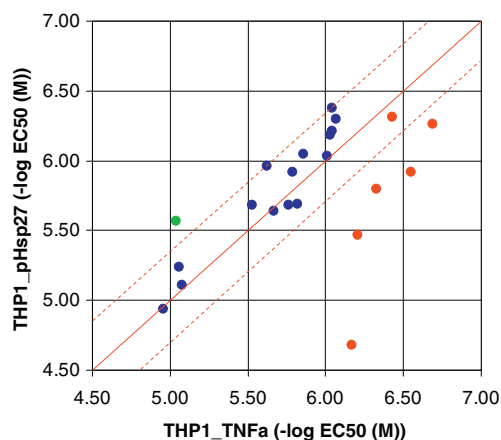


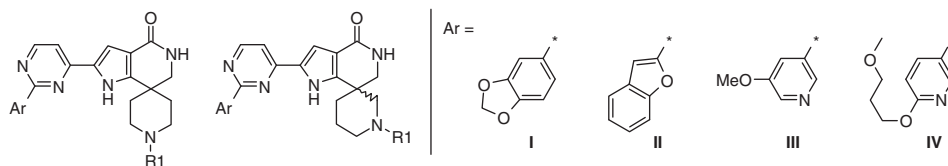
Figure 2. Correlation Hsp27 phosphorylation (pHsp27) and TNFα production in THP1 cells. Solid red line indicates equi-potency and dotted indicate a 2-fold difference. The red dots represent the benzofuranyl series and the green dot is the reference compound PH-089.

enantiomerically pure 3-piperidyl analogues were prepared via separation at the chloropyrimidine intermediate stage by means of chiral preparative HPLC.¹⁰ Finally, enantiomerically pure target compounds (ee >99%) were prepared as described for the racemic 3-piperidyl inhibitors and as outlined in Scheme 1. Using vibrational circular dichroism (VCD) experiments we were able to deter-

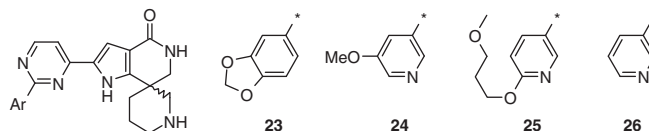
mine the absolute configuration of each of the stereoisomers of **23**.¹¹ In line with our expectations, the *S*-configuration could be traced back to first eluting stereoisomer 1, and the optical antipode to stereoisomer 2 of the common intermediate. In all chiral pairs biochemical potency could be attributed to the (*S*)-stereoisomer, and for the majority of racemic mixtures and isolated stereoisomers, the biochemical and cellular activities correlate well (Table 3). Compound **24** is an exception, possibly because the cellular potency of the enantiomers and the racemate are in the same range, but in this case the biochemical potency failed to correlate with pHsp27 and TNFα data. With their sub-micromolar cellular activities, (*S*)-**23** and (*S*)-**25** have the most attractive overall profile. Moreover, it is anticipated that (*S*)-**23** will have similar oral bioavailability as its racemate.

In computational models of MK2 and MK3—which was previously described as a suitable model for MK2 with a near-identical active site¹²—compound (*S*)-**23** is almost perfectly aligned with **1** in X-ray structures of, respectively, MK2:**1** and MK3:**1**,⁶ with the obvious exception of the interactions involving the basic amine (Fig. 3). In the *S*-configuration of the 3-piperidyl ring, the nitrogen can be positioned within hydrogen-bond distance of the main chain carbonyl of Glu190 (Glu170 in MK3 numbering) and close to the side chain of Asn191/Asn171, and this is not possible for the (*R*)-**23**.

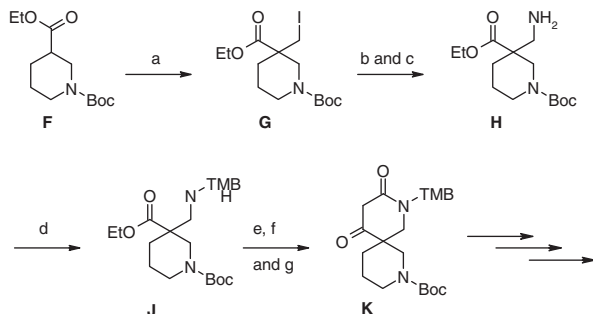
Given the good correlation between the pHsp27 and TNFα data generated for this chemical series, we inferred that potential off-target kinase inhibition should not intervene with the observed

Table 2
pK_a, Caco-2 and oral exposure relationship

Compd	Spiro	Ar	R1	MK2 IMAP EC ₅₀ ^a (nM)	Caco-2 nm/s	pK _a ^b (pH 7.4)	HLM/RLM (t ^{1/2} min)	AUC rat (μM h)	c Log P
1	4-Piperidyl	I	H	4.3	1	9.3	>60/>60	<0.006	1.7
3a	4-Piperidyl	II	H	5.9	0	9.1	>60/>60	<0.006	2.4
3b	4-Piperidyl	II	Me	13	10	8.1	>60/>60	0.078	2.8
3c	4-Piperidyl	II	Et	59	8	8.6	>60/>59.6	0.154	3.4
22	3-Piperidyl	II	H	11	15	8.4	>60/>60	0.472	2.8
23	3-Piperidyl	I	H	28	34	8.3	>60/48.5	3.210	2.0
24	3-Piperidyl	III	H	24	20	8.4	56.7/42.1	NT ^c	1.0
25	3-Piperidyl	IV	H	21	42	8.2	>60/>60	0.882	1.7

^{a-c} See Table 1.^b Experimentally determined pK_a values at pH 7.4.**Table 3**
Inhibitory MK2 activity of compounds **23–26**

Compd	Stereoisomer ^a	MK2 IMAP EC ₅₀ ^b (nM)	pHsp27 EC ₅₀ ^c (μM)	TNFα-THP1 EC ₅₀ ^b (μM)	TNFα-PBMC EC ₅₀ ^e (μM)
23	<i>Rac.</i>	28	0.93	1.4	1.1
(<i>S</i>)- 23	1	7.4	0.50	0.85	0.45
(<i>R</i>)- 23	2	91	7.7	8.3	3.0
24	<i>Rac.</i>	24	0.9	1.4	1.0
(<i>S</i>)- 24	1	9.3	1.1	2.4	1.3
(<i>R</i>)- 24	2	126	2.3	2.2	>10
25	<i>Rac.</i>	21	1.4	1.5	0.92
(<i>S</i>)- 25	1	6.9	0.40	0.98	0.43
(<i>R</i>)- 25	2	129	>10	>10	6.9
26	<i>Rac.</i>	18	2.1	3.0	3.3
(<i>S</i>)- 26	1	6.5	1.2	1.6	0.93
(<i>R</i>)- 26	2	288	5.8	8.7	4.3

^a Stereoisomers separated by chiral preparative HPLC on the chloropyrimidine intermediate.^{b-d} See Table 1.^e hPBMC's are pre-incubated for 30 min with MK2 inhibitors (duplicates for each dilution) prior to stimulation with LPS. Four hours following LPS induction culture medium is withdrawn from the cells for TNFα measurements.⁹

Scheme 2. Reagents and conditions: (a) diiodomethane, LDA, THF -78°C to rt (87%); (b) NaN₃, DMSO, 70°C (69%); (c) Pd(OH)₂, H₂(g), EtOH, rt, (97%); (d) 2,4,6-trimethoxybenzaldehyde, NaBH(OAc)₃, EtOH, rt (100%); (e) ClCOCH₂COOMe, DMAP, pyridine, DCM, rt (94%); (f) NaOMe, MeOH, 60°C (91%); (g) ACN/H₂O (1:1) 80°C (46%).

inhibition of cytokine production in THP1 cells and PBMCs (Table 3). None of the tested compounds inhibited upstream kinase p38. Yet, Millipore profiling on 233 kinases revealed a number of other

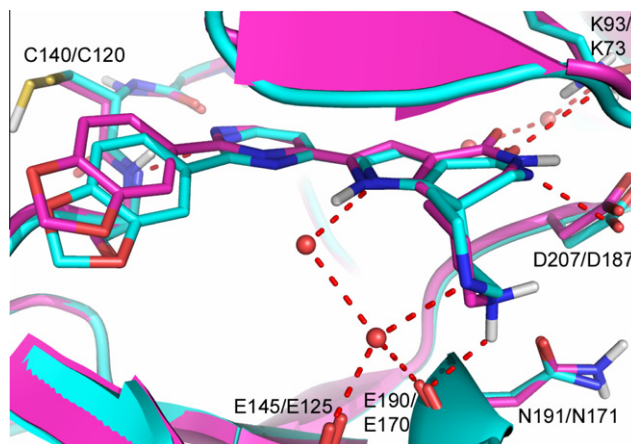


Figure 3. Overlay of an X-ray structure of **1** (cyan) and a computational model of the (*S*)-enantiomer of 3-piperidyl analogue **23** (magenta) bound to MK3. Numbering is consistent with the sequences of MK2/MK3. Similar structures and models were generated for **1** and **23** bound to MK2 (not shown).

kinases that were substantially inhibited. At 1 μM , 16 out of 233 kinases were inhibited $\geq 95\%$ by **1**. Benzofuranyl derivative **3a** was less selective which aids to the conclusion that its anti-TNF α effects are apparently not only mediated by MK2. This also demonstrates that the front pocket substitution has significant impact on overall selectivity observed in kinase panels. 3-Piperidyl analogues **23–25** exhibited much higher selectivity in kinase panels. For instance, compounds **23** and **24** showed $\geq 95\%$ inhibition of only two kinases at 1 μM next to potent blockade of MK2, MK3, and MK5. Inhibition of both MK3 and MK5 will most likely contribute to the observed cellular effects, since they share common functions towards downstream events.¹³ Other kinases that are substantially inhibited ($\geq 80\%$ at 1 μM) by all tested compounds in this series are PIM1&3, DRAK1, ERK1&2, and CHK2. The inhibition of these kinases will need special attention in future optimization cycles.

In summary, simply moving the piperidyl nitrogen from the four to the three position provided an MK2 inhibitor series that matched the desired preclinical profile. In doing so, the oral bioavailability in rodents improved dramatically to acceptable exposure levels. The lower pK_a of the basic amine appears to be of paramount importance to achieve this. Chiral separation and analysis identified the most active (*S*)-enantiomer. The *in vivo* efficacy following oral administration of these enantiomerically pure 3-piperidyl analogues in preclinical arthritis models will be the subject of future investigations.

Acknowledgments

We thank Dr. Hans van Eenennaam and Dr. Rob Nelissen for the valuable discussions regarding the MK2 program. BioTools is acknowledged for the absolute configuration determination studies.

References and notes

- Saklatvala, J. *Curr. Opin. Pharmacol.* **2004**, *4*, 372.
- (a) Sweeney, S. E. *Nat. Rev. Rheumatol.* **2009**, *5*, 475; (b) Hammaker, D.; Firestein, G. S. *Ann. Rheum. Dis.* **2010**, *69*, i77; (c) Cheung, P. C. F.; Campbell, D. G.; Nebreda, A. R.; Cohen, P. *EMBO J.* **2003**, *22*, 5793.
- (a) Kotlyarov, A.; Neiningger, A.; Schubert, C.; Eckert, R.; Birchmeier, C.; Volk, H. D.; Gaestel, M. *Nat. Cell. Biol.* **1999**, *1*, 94; (b) Hegen, M.; Gaestel, M.; Nickerson-Nutter, C. L.; Lin, L.-L.; Telliez, J.-B. *J. Immunol.* **2006**, *177*, 1913.
- Schlapbach, A.; Huppertz, C. *Future Med. Chem.* **2009**, *1*, 1243.
- Anderson, D. R.; Meyers, M. J.; Vernier, W. F.; Mahoney, M. W.; Kurumbail, R. G.; Caspers, N.; Poda, G. I.; Schindler, J. F.; Reitz, D. B.; Mourey, R. J. *J. Med. Chem.* **2007**, *50*, 2647.
- Barf, T.; Kaptein, A.; Wilde, S. de; Heijden, R. van der; Someren, R. van; Demont, D.; Schultz-Fademrecht, C.; Versteegh, J.; Zeeland, M. van; Seegers, N.; Kazemier, B.; Kar, B. van de; Hoek, M. van; Roos, J. de; Klop, H.; Smeets, R.; Hofstra, C.; Hornberg, J.; Oubrie, A. *Bioorg. Med. Chem. Lett.* **2011**. Accepted for publication.
- Pyrane analogue **2** was essentially prepared as described for the 4-piperidyl compounds, starting with methyl 4-aminomethyl-tetrahydro-pyran-4-carboxylate.
- THP1 cells are seeded at 1.5×10^5 cells per well in DMEM F12 (Gibco) supplemented with Penicillin/Streptomycin (80 U/mL; 80 $\mu\text{g}/\text{mL}$) and 10% FBS (Fetal Bovine Serum) in 96 well plate. Cells are left to rest for at least 18 h in a humidified atmosphere at 5–7% CO_2 at 37 $^\circ\text{C}$, prior to incubation with test compounds. Dilutions of test compounds in DMSO (0.1% DMSO final concentration in assay) are added to the cells. Following a 60-min incubation LPS is added (final LPS concentration 10 $\mu\text{g}/\text{mL}$). Following a 60 min incubation cells are harvested and lysed for the measurement of total and phosphorylated Hsp27 (pHsp27). Total Hsp27 and pHsp27 are quantified using the Multi-Spot assay from Meso Scale according to protocol.
- PBMCs are isolated from buffy coats from human blood and are seeded at 2.5×10^5 cells per well in DMEM F12 (Gibco) supplemented with Penicillin/Streptomycin (80 U/mL; 80 $\mu\text{g}/\text{mL}$) and 10% FBS (Fetal Bovine Serum) in 96 well plate. Cells are left to rest for at least 1 h, prior to incubation with test compounds. Dilutions of test compounds in DMSO (0.1% DMSO final concentration in assay) are added to the cells. Following a 30 min incubation LPS is added (final LPS concentration 10 $\mu\text{g}/\text{mL}$). Following a 4 h incubation at 5–7% CO_2 at 37 $^\circ\text{C}$ in humidified atmosphere, culture medium is collected for the measurement of TNF α . The amount of TNF α in the culture medium is quantified by ELISA using HuTNF α assay from Cytoset according to protocol.
- Separation of enantiomers was effected at the chloropyrimidine stage on a Chiralpack AD-H column (20 \times 250 mm, particle size 5 μm), eluting with heptane/IPA (80/20 v/v). Stereoisomer 1 eluted at 15.8 min, and stereoisomer 2 at 27.8 min. *Ee*'s were $>99\%$ as determined with analytical chiral chromatography.
- Vibrational Circular Dichroism (VCD) configuration determination of the stereoisomers of **23**: Samples (7.6 mg each) were dissolved in 0.2 mL DMSO- d_6 and placed in a cell with 100 μm pathlength and BaF $_2$ windows. IR and VCD spectra were recorded on a Chiral IR2XTM VCD spectrometer from BioTools, Inc., equipped with DualPEM accessories. The instrument was optimized at 1400 cm^{-1} . Spectra were collected for 8 h (stereoisomer 1) and 15 h (stereoisomer 2) with 4 cm^{-1} resolution. Calculations: A model of the (*S*)-configuration was built and a conformational search was carried out with Hyperchem (Hypercube, Inc., Gainesville, FL, USA) for the entire structure at the molecular mechanics level. Geometry optimization, frequency, IR and VCD intensity calculations of 47 conformers, which resulted from the conformational search, were carried out at the DFT level (B3LYP functional/6-31G(d) basis set) with GAUSSIAN 09 (Gaussian Inc., Wallingford, CT). The four lowest-energy conformers were used for calculating the averaged VCD and IR spectra. The configurations were assigned by spectral comparison of experimental and calculated spectra.
- Cheng, R.; Felicetti, B.; Palan, S.; Toogood-Johnson, I.; Scheich, C.; Barker, J.; Whittaker, M.; Hestekamp, T. *Protein Sci.* **2010**, *19*, 168.
- (a) Ronkina, N.; Kotlyarov, A.; Dittrich-Breiholz, O.; Kracht, M.; Hitti, E.; Milarski, K.; Askew, R.; Marusic, S.; Lin, L.-L.; Gaestel, M.; Telliez, J.-B. *Mol. Cell. Biol.* **2007**, *27*, 170; (b) New, L.; Jiang, Y.; Zhao, M.; Liu, K.; Zhu, W.; Flood, L. J.; Kato, Y.; Parry, G. C. N.; Han, J. *EMBO J.* **1998**, *17*, 3372.